Mathematical Medicine and Biology: A Journal of the IMA (2020) **37**, 313–333
doi:10.1093/imammb/dqz016
Advance Access publication on 8 December 2019

Allostery in oligomeric receptor models

Gregory Douglas Conradi Smith*
Department of Applied Science, Neuroscience Program Faculty Affiliate, William & Mary, Williamsburg, VA 23187, USA
*Corresponding author. E-mail: greg@wm.edu

[Received on 7 May 2019; revised on 3 October 2019; accepted on 22 October 2019]

We show how equilibrium binding curves of receptor homodimers can be expressed as rational polynomial functions of the equilibrium binding curves of the constituent monomers, without approximation and without assuming independence of receptor monomers. Using a distinguished spanning tree construction for reduced graph powers, the method properly accounts for thermodynamic constraints and allosteric interactions between receptor monomers (i.e. conformational coupling). The method is completely general; it begins with an arbitrary undirected graph representing the topology of a monomer state-transition diagram and ends with an algebraic expression for the equilibrium binding curve of a receptor oligomer composed of two or more identical and indistinguishable monomers. Several specific examples are analysed, including guanine nucleotide-binding protein-coupled receptor dimers and tetramers composed of multiple 'ternary complex' monomers.

Keywords: pharmacological receptor models; allosteric modulation; product graphs.

1. Introduction

Guanine nucleotide-binding protein (G protein)-coupled receptors (GPCRs) are the largest family of signalling proteins in the mammalian genome and targets for therapeutic drugs (Audet & Bouvier, 2012; Rosenbaum *et al.*, 2009). When GPCRs are activated by extracellular agonists, they interact with heterotrimeric G proteins to regulate downstream second messenger and protein kinase cascades, notably, cyclic-adenosine monophosphate, inositol 1,4,5-triphosphate and diacylglycerol.

Equilibrium receptor models are used by pharmacologists to quantify changes in ligand affinity and efficacy, and various modes of activation of GPCRs, and to clarify mechanistic hypotheses regarding drug action (Giraldo, 2012; Gregory *et al.*, 2010; Hall, 2012; Kenakin, 2016; May *et al.*, 2007; Wang *et al.*, 2018). Pharmaceuticals that allosterically modulate GPCRs are of therapeutic interest due to their potential for greater subtype specificity than orthosteric ligands (Engers & Lindsley, 2013; Gregory *et al.*, 2013). Indeed, allosteric modulators hold promise for treating numerous CNS disorders (Conn *et al.*, 2009; Foster & Conn, 2017; O'Brien & Conn, 2016; Terrillon & Bouvier, 2004).

Evidence for dimerization and oligomerization of GPCRs has been obtained using various experimental methods, including radioligand binding, coimmunoprecipitation and fluorescence resonance energy transfer microscopy (Kaczor & Selent, 2011; Levitz *et al.*, 2016; Park *et al.*, 2008). It is widely believed that dimerization and higher-order complexing (oligomerization) of GPCRs are common phenomena that diversify GPCR signaling and opportunities for pharmacological intervention (Bouvier, 2001; Ferré *et al.*, 2014; Gaitonde & González-Maeso, 2017; González-Maeso, 2011; Kenakin, 2014; Milligan & Smith, 2007; Milligan *et al.*, 2019; Park & Palczewski, 2005).

GPCR dimerization may involve identical receptors (homodimerization), two different subtypes of the same family or receptors from distantly related families (heterodimerization). Several family C GPCRs exist and function as covalently linked homodimers (e.g. metabotropic glutamate receptors and calcium-sensing receptors) (Niswender & Conn, 2010). Some family A GPCRs (e.g. β_1-adenosine and dopamine D_2 receptors) function as homodimers (González-Maeso, 2014). Some GPCRs are obligate heterodimers (e.g. the $GABA_B$ receptor and taste receptors for sweet and umami responses) (Chandrashekar *et al.*, 2006; Marshall *et al.*, 1999; Pin *et al.*, 2004). A prototypical GPCR heteromer (composed of receptors from different families) is formed by A_{2A} adenosine receptors and D_2 dopamine receptors (Borroto-Escuela *et al.*, 2018; Ferré *et al.*, 2004; Fuxe *et al.*, 2010).

In many of the above examples, physical interactions between subunits of GPCR oligomers are known, or suspected to be, important determinants in the mechanism of receptor activation (Ferré, 2015; Goudet *et al.*, 2005; Kubo & Tateyama, 2005; Palczewski, 2010; Pin & Bettler, 2016; Vischer *et al.*, 2015). Mathematical analyses have provided specific insights into interactions between subunits of receptor oligomers, i.e. conformational coupling (Casadó *et al.*, 2007; Christopoulos & Kenakin, 2002; Durroux, 2005; Farran, 2017; Park *et al.*, 2004; Rovira *et al.*, 2009). However, a deeper theoretical understanding of oligomeric signalling is needed. In response to this need, we have developed a novel theoretical framework for understanding allosteric interactions and thermodynamic constraints within oligomeric receptors that are composed of any number of identical monomers. The framework allows equilibrium binding curves of receptor dimers to be expressed in terms of the properties of constituent monomers, without approximation and without assuming independence of receptor monomers.

This paper presumes understanding of receptor modelling and mathematical concepts familiar to the mainstream pharmacological community; see Kenakin (2018) for an overview. Section 2 reviews this methodology and introduces helpful notation that was developed as part of this work. *En passant*, we distinguish two ways that thermodynamic constraints and allosteric parameters arise in receptor models: (1) when the state-transition graph of a receptor includes cycles and (2) as a property of receptor oligomers that emerges via conformational coupling of constituent monomers.

2. Thermodynamic constraints and allosteric parameters in the ternary complex model

It is well known that G proteins may modulate ligand affinity at GPCRs (De Lean *et al.*, 1980; Ehlert, 2000; Kenakin, 2004; Maguire *et al.*, 1976; Weiss *et al.*, 1996). We review this phenomenon to illustrate the relationship between cycles in the graph representing receptor model topology, thermodynamic constraints on equilibrium model parameters and allosteric coupling (Hill, 1985).

Consider the well-known ternary complex model of interactions between a 7-transmembrane receptor (R), endogenous ligand (L) and heterotrimeric G protein (Fig. 1a). This model hypothesizes distinct binding sites for ligand (orthosteric) and G protein (allosteric), four receptor conformations (states) and four reversible reactions. Microscopic reversibility requires that the product of the transition rates (not shown) around the four states of the ternary complex model is the same clockwise as counter-clockwise for fixed ligand and G protein concentrations (Hill, 1989). If we consider bimolecular association as the forward reaction, then the chemical equilibrium constants are $K_L = [LR]/([L][R])$, $K_G = [RG]/([G][R])$, $\hat{K}_L = [LRG]/([L][RG])$ and $\hat{K}_G = [LRG]/([G][LR])$, where [L], [R] etc. represent equilibrium concentrations. The cycle in the ternary complex model leads to the thermodynamic constraint $K_L\hat{K}_G = K_G\hat{K}_L$ and, consequently, the ternary complex model has three (not four) free equilibrium parameters. To emphasize the cooperativity of the two binding processes, one may define an allosteric parameter $\gamma = \hat{K}_G/K_G = \hat{K}_L/K_L$. In that case, the receptor model is specified by two association constants (K_L, K_G) and γ, the strength of allosteric coupling. The ligand affinity is

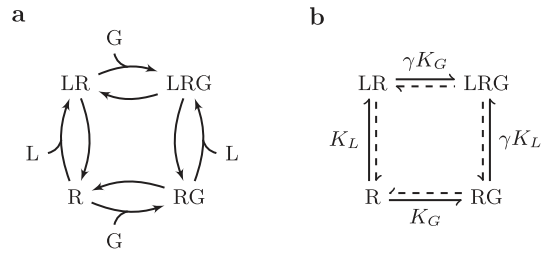

FIG. 1. Ternary complex model of a G protein-coupled receptor (De Lean *et al.*, 1980; Ehlert, 2000; Kenakin, 2004; Maguire *et al.*, 1976; Weiss *et al.*, 1996). For given ligand and G protein concentration ([L] and [G]), there are three free equilibrium parameters: two association constants (K_L, K_G) and the allosteric parameter γ.

K_L when G protein is unbound and γK_L when G protein is bound. Thus, $\gamma > 1$ implies that G protein binding increases agonist affinity, as observed for β_2-ARs (De Lean *et al.*, 1980; Maguire *et al.*, 1976; Weiss *et al.*, 1996).

For any [L] and [G], the equilibrium fraction of receptors in each of the four states of the ternary complex model (Fig. 1) can be found by expressing each receptor state concentration in terms of [R],

$$[\mathrm{LR}] = K_L[\mathrm{L}][\mathrm{R}]$$
$$[\mathrm{RG}] = K_G[\mathrm{G}][\mathrm{R}]$$
$$[\mathrm{LRG}] = \gamma K_G[\mathrm{G}][\mathrm{LR}] = \gamma K_G[\mathrm{G}]K_L[\mathrm{L}][\mathrm{R}].$$

Solving these equations simultaneously with the equation for the conserved total receptor concentration, namely,

$$[\mathrm{R}]_T = [\mathrm{R}] + [\mathrm{LR}] + [\mathrm{RG}] + [\mathrm{LRG}]\,,$$

gives the fraction of receptors in each state,

$$[\mathrm{R}]/[\mathrm{R}]_T = 1/z_T \tag{2.1}$$

$$[\mathrm{LR}]/[\mathrm{R}]_T = K_L[\mathrm{L}]/z_T \tag{2.2}$$

$$[\mathrm{RG}]/[\mathrm{R}]_T = K_G[\mathrm{G}]/z_T \tag{2.3}$$

$$[\mathrm{LRG}]/[\mathrm{R}]_T = \gamma K_G[\mathrm{G}]K_L[\mathrm{L}]/z_T \tag{2.4}$$

where $z_T = 1 + K_L[\mathrm{L}] + K_G[\mathrm{G}] + \gamma K_G[\mathrm{G}]K_L[\mathrm{L}]$. Figure 2 shows example binding curves for the ternary complex model.

3. Cooperativity and constraints in receptor dimers

The previous section illustrated the well-known phenomena of allosteric coupling in the ternary complex model. Less well known is how thermodynamic constraints and allosteric parameters arise as an

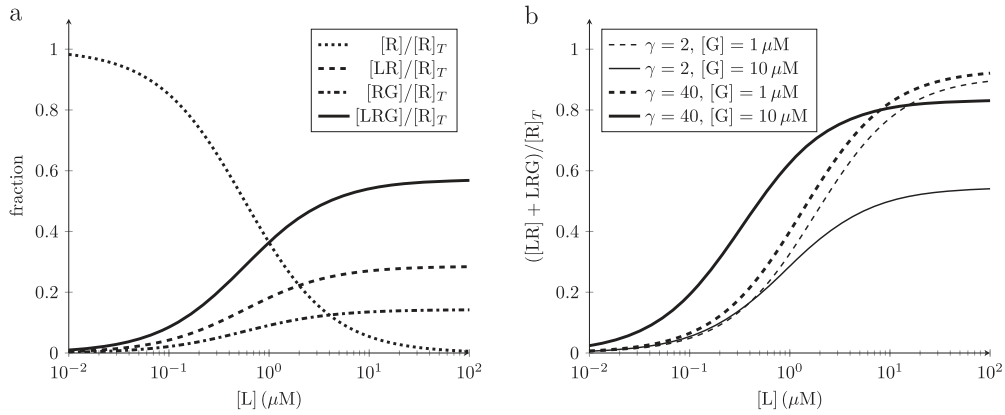

FIG. 2. Example binding curves for ternary complex monomer (2.1)–(2.4). Parameters: $K_L = 0.5\,\mu\text{M}^{-1}$, $K_G = 0.1\,\mu\text{M}^{-1}$ and in (a) [G] = 5 μM and $\gamma = 40$.

emergent properties of receptor dimerization. To demonstrate this phenomenon, consider a model receptor monomer with three states and two sequential binding reactions,

$$a \underset{\overbrace{\kappa_{\mathsf{b}}^* x}^{\kappa_{\mathsf{b}}}}{\rightleftharpoons} b \underset{\overbrace{\kappa_{\mathsf{c}}^* x}^{\kappa_{\mathsf{c}}}}{\rightleftharpoons} c \tag{3.1}$$

In the state-transition diagram shown above, κ_{b} and κ_{c} are dimensionless equilibrium constants, κ_{b}^* and κ_{c}^* are association constants and x is ligand concentration. The solid harpoons indicate the forward reaction direction. For example, the reaction labelled κ_{b} has a as reactant and b as product; consequently, increasing κ_{b} decreases the equilibrium probability (relative fraction) of state a and increases the probability of state b. The three states of (3.1) are labelled so that the reactant comes before the product in dictionary order (a to b to c). The subscript of the equilibrium constants κ_{b} and κ_{c} are chosen to match the label of the reaction products.

For an isolated monomer with state-transition diagram given by (3.1), the probability of state i is given by $\pi_i = z_i/z_T$, where $z_T = \sum_i z_i$, $z_a = 1$, $z_b = \kappa_{\mathsf{b}} = \kappa_{\mathsf{b}}^* x$ and $z_c = \kappa_{\mathsf{b}}\kappa_{\mathsf{c}} = \kappa_{\mathsf{b}}^*\kappa_{\mathsf{c}}^* x^2$. That is,

$$\pi_a = \frac{1}{1 + \kappa_{\mathsf{b}}^* x + \kappa_{\mathsf{b}}^*\kappa_{\mathsf{c}}^* x^2}, \quad \pi_b = \frac{\kappa_{\mathsf{b}}^* x}{1 + \kappa_{\mathsf{b}}^* x + \kappa_{\mathsf{b}}^*\kappa_{\mathsf{c}}^* x^2} \quad \text{and} \quad \pi_c = \frac{\kappa_{\mathsf{b}}^*\kappa_{\mathsf{c}}^* x^2}{1 + \kappa_{\mathsf{b}}^* x + \kappa_{\mathsf{b}}^*\kappa_{\mathsf{c}}^* x^2}. \tag{3.2}$$

It is helpful to present this set of rational functions using the following compact notation:

$$[\pi_a : \pi_b : \pi_c] = [1 : \kappa_{\mathsf{b}} : \kappa_{\mathsf{b}}\kappa_{\mathsf{c}}] = \left[1 : \kappa_{\mathsf{b}}^* x : \kappa_{\mathsf{b}}^*\kappa_{\mathsf{c}}^* x^2\right].$$

In expressions of this kind, it is understood that $[x_1 : x_2 : \cdots : x_n] = [\lambda x_1 : \lambda x_2 : \cdots : \lambda x_n]$ for any $\lambda \neq 0$. Furthermore, $\lambda = 1/\sum_i x_n$ gives the probability distribution $\pi = (\pi_1, \pi_2, \ldots, \pi_n)$ where $1 = \sum_i \pi_i$.

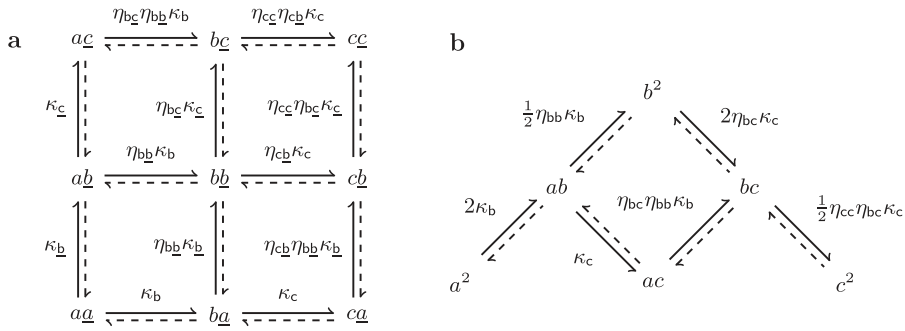

FIG. 3. (a) Equilibrium parameters for a heterodimer composed of two 3-state monomers (same topology and different parameters). There are four 4-cycles and four allosteric parameters: $\eta_{\mathsf{b}\underline{\mathsf{b}}}$, $\eta_{\mathsf{b}\underline{\mathsf{c}}}$, $\eta_{\mathsf{c}\underline{\mathsf{b}}}$ and $\eta_{\mathsf{c}\underline{\mathsf{c}}}$. (b) State-transition diagrams for a dimer composed of identical and indistinguishable subunits (not necessarily independent) and three allosteric parameters: η_{bb}, η_{bc} and η_{cc}.

3.1 *Receptor dimer composed of distinguishable monomers*

A receptor dimer model composed of two distinguishable monomers with the 3-state topology of (3.1) has $3^2 = 9$ states, 12 reversible reactions, 4 thermodynamic constraints and $12 - 4 = 8$ free equilibrium parameters (Fig. 3a). Each monomer contributes two parameters, for a total of four (κ_{b}, κ_{c} for one monomer and $\kappa_{\underline{\mathsf{b}}}$, $\kappa_{\underline{\mathsf{c}}}$ for the other monomer). The remaining parameters, denoted $\eta_{\mathsf{b}\underline{\mathsf{b}}}$, $\eta_{\mathsf{b}\underline{\mathsf{c}}}$, $\eta_{\mathsf{c}\underline{\mathsf{b}}}$ and $\eta_{\mathsf{c}\underline{\mathsf{c}}}$ in Fig. 3a, encode the strength of the four possible allosteric interactions among the monomers; there is one allosteric parameter for each 4-cycle, as in the ternary complex model (Fig. 1).

To clarify the meaning of the emergent allosteric parameters shown in Fig. 3a, let us write $\kappa_{\mathsf{b}}[\underline{a}]$ for the equilibrium constant of the $a \rightleftharpoons b$ reaction of first monomer occurring in the context of the second monomer being in state $\underline{a}$ and similarly for $\kappa_{\mathsf{b}}[\underline{b}]$, $\kappa_{\underline{\mathsf{b}}}[a]$, $\kappa_{\underline{\mathsf{b}}}[b]$ (below left).

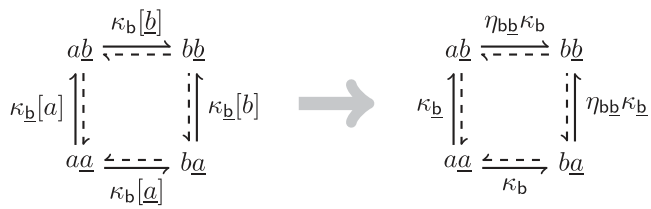

In that case, the allosteric parameter $\eta_{\mathsf{b}\underline{\mathsf{b}}}$ is, by definition,

$$\eta_{\mathsf{b}\underline{\mathsf{b}}} := \frac{\kappa_{\mathsf{b}}[\underline{b}]}{\kappa_{\mathsf{b}}[\underline{a}]} = \frac{\kappa_{\underline{\mathsf{b}}}[b]}{\kappa_{\underline{\mathsf{b}}}[a]}\,.$$

That is, $\eta_{\mathsf{b}\underline{\mathsf{b}}}$ is the degree to which κ_{b}, the equilibrium constant of process b (the $a \rightleftharpoons b$ transition in monomer 1) increases upon the occurrence of process $\underline{\mathsf{b}}$ (the $\underline{a} \rightleftharpoons \underline{b}$ transition in monomer 2).

Taking states a and $\underline{a}$ as reference states, we write $\kappa_{\mathsf{b}} := \kappa_{\mathsf{b}}[\underline{a}]$, $\kappa_{\underline{\mathsf{b}}} := \kappa_{\underline{\mathsf{b}}}[a]$. Consequently, $\kappa_{\mathsf{b}}[\underline{b}] = \eta_{\mathsf{b}\underline{\mathsf{b}}}\kappa_{\mathsf{b}}$, $\kappa_{\underline{\mathsf{b}}}[b] = \eta_{\mathsf{b}\underline{\mathsf{b}}}\kappa_{\underline{\mathsf{b}}}$, leading to the choice of parameters for the 4-cycle shown above right. Similar definitions for $\eta_{\mathsf{b}\underline{\mathsf{c}}}$, $\eta_{\mathsf{c}\underline{\mathsf{b}}}$ and $\eta_{\mathsf{c}\underline{\mathsf{c}}}$ lead to the 9-state model of Fig. 3a. The proportion of dimers in each

state,

$$\pi = [z_{a\underline{a}} : z_{a\underline{b}} : z_{b\underline{a}} : z_{a\underline{c}} : z_{b\underline{b}} : z_{c\underline{a}} : z_{b\underline{c}} : z_{c\underline{b}} : z_{c\underline{c}}],$$

can be 'read off' the state-transition diagram, remembering that the equilibrium constants are defined so that $a \to b \to c$ and $\underline{a} \to \underline{b} \to \underline{c}$ are forward reactions. Because $a\underline{a}$ is not a product of a forward reaction, we assign $z_{a\underline{a}} = 1$. The other z_i are given by the product of parameters labelling forward reactions on a path from $a\underline{a}$ to i. For example, to calculate $z_{c\underline{b}}$, we observe the path $a\underline{a} \to a\underline{b} \to b\underline{b} \to c\underline{b}$, passes in the forward direction through three reactions with equilibrium constants $\kappa_{\underline{\mathsf{b}}}$ ($a\underline{a} \to a\underline{b}$), $\eta_{\mathsf{b}\underline{\mathsf{b}}}\kappa_{\mathsf{b}}$ ($a\underline{b} \to b\underline{b}$) and $\eta_{\mathsf{c}\underline{\mathsf{b}}}\kappa_{\mathsf{c}}$ ($b\underline{b} \to c\underline{b}$); the product gives $z_{c\underline{b}} = \eta_{\mathsf{c}\underline{\mathsf{b}}}\kappa_{\mathsf{c}} \cdot \eta_{\mathsf{b}\underline{\mathsf{b}}}\kappa_{\mathsf{b}} \cdot \kappa_{\underline{\mathsf{b}}}$. In a similar manner, we obtain $z_{b\underline{a}} = \kappa_{\mathsf{b}}$, $z_{a\underline{b}} = \kappa_{\underline{\mathsf{b}}}$, $z_{c\underline{a}} = \kappa_{\mathsf{c}} \cdot \kappa_{\mathsf{b}}$, $z_{b\underline{b}} = \eta_{\mathsf{b}\underline{\mathsf{b}}}\kappa_{\mathsf{b}} \cdot \kappa_{\underline{\mathsf{b}}}$, $z_{a\underline{c}} = \kappa_{\underline{\mathsf{c}}} \cdot \kappa_{\underline{\mathsf{b}}}$,

$$z_{b\underline{c}} = \eta_{\mathsf{b}\underline{\mathsf{c}}}\kappa_{\underline{\mathsf{c}}} \cdot \eta_{\mathsf{b}\underline{\mathsf{b}}}\kappa_{\underline{\mathsf{b}}} \cdot \kappa_{\mathsf{b}}$$

$$z_{c\underline{c}} = \eta_{\mathsf{c}\underline{\mathsf{c}}}\eta_{\mathsf{c}\underline{\mathsf{b}}}\kappa_{\mathsf{c}} \cdot \eta_{\mathsf{b}\underline{\mathsf{c}}}\eta_{\mathsf{b}\underline{\mathsf{b}}}\kappa_{\mathsf{b}} \cdot \kappa_{\underline{\mathsf{c}}} \cdot \kappa_{\underline{\mathsf{b}}}.$$

3.2 *Receptor dimer composed of indistinguishable monomers*

A receptor homodimer composed of two indistinguishable monomers with the 3-state topology of (3.1) has six states, six reversible reactions, one thermodynamic constraint and $6 - 1 = 5$ free equilibrium parameters (see Fig. 3b). The homodimer state-transition diagram (Fig. 3b) is a contraction of the heterodimer diagram (Fig. 3a) obtained by lumping and renaming states ($a\underline{a} \to a^2$, $b\underline{a} + a\underline{b} \to ab, \ldots$) and identifying parameters ($\kappa_{\mathsf{b}} = \kappa_{\underline{\mathsf{b}}}$, $\kappa_{\mathsf{c}} = \kappa_{\underline{\mathsf{c}}}$, $\eta_{\mathsf{b}\underline{\mathsf{c}}} = \eta_{\mathsf{c}\underline{\mathsf{b}}}$). The monomers, being identical, contribute only two parameters (κ_{b}, κ_{c}) to the homodimer state-transition diagram (Fig. 3b). For a receptor dimer composed of indistinguishable monomers (Fig. 3b), there are three allosteric parameters, denoted η_{bb}, η_{bc} and η_{cc}:

$$\eta_{\mathsf{bb}} := \frac{\kappa_{\mathsf{b}}[b]}{\kappa_{\mathsf{b}}[a]} \qquad \eta_{\mathsf{bc}} := \frac{\kappa_{\mathsf{b}}[c]}{\kappa_{\mathsf{b}}[b]} = \frac{\kappa_{\mathsf{c}}[b]}{\kappa_{\mathsf{c}}[a]} \qquad \eta_{\mathsf{cc}} := \frac{\kappa_{\mathsf{c}}[c]}{\kappa_{\mathsf{c}}[b]} \qquad .$$

For example, η_{bc} is the degree to which κ_{b}, the equilibrium constant of process b (the $a \rightleftharpoons b$ transition) increases upon the occurrence of process c (the $b \rightleftharpoons c$ transition) in the other monomer. The relative probability of dimers in each state,

$$\pi = [z_{a^2} : z_{ab} : z_{b^2} : z_{ac} : z_{bc} : z_{c^2}], \tag{3.3}$$

is given by $z_{a^2} = 1$, $z_{ab} = 2\kappa_{\mathsf{b}}$, $z_{b^2} = \eta_{\mathsf{bb}}\kappa_{\mathsf{b}}^2$, $z_{ac} = 2\kappa_{\mathsf{b}}\kappa_{\mathsf{c}}$,

$$z_{bc} = \eta_{\mathsf{bc}}\eta_{\mathsf{bb}}\kappa_{\mathsf{c}} \cdot \kappa_{\mathsf{c}} \cdot 2\kappa_{\mathsf{b}} = 2\eta_{\mathsf{bb}}\eta_{\mathsf{bc}}\kappa_{\mathsf{b}}^2\kappa_{\mathsf{c}}$$

$$z_{c^2} = \tfrac{1}{2}\eta_{\mathsf{cc}}\eta_{\mathsf{bc}}\kappa_{\mathsf{c}} \cdot \eta_{\mathsf{bc}}\eta_{\mathsf{bb}}\kappa_{\mathsf{b}} \cdot \kappa_{\mathsf{c}} \cdot 2\kappa_{\mathsf{b}} = \eta_{\mathsf{bb}}\eta_{\mathsf{bc}}^2\eta_{\mathsf{cc}}\kappa_{\mathsf{b}}^2\kappa_{\mathsf{c}}^2,$$

where the combinatorial coefficient 2 (resp. 1/2) appears as a factor on the transitions out of (resp. into) states a^2, b^2 and c^2. Note that this calculation does not assume independent monomers. Rather, the dependence of the monomers in the homodimer has been parameterized by the three allosteric parameters η_{bb}, η_{bc} and η_{cc}. To see this, transform (3.3) to an equivalent expression by dividing each term by $(1 + \kappa_{\mathsf{b}} + \kappa_{\mathsf{c}}\kappa_{\mathsf{b}})^2$ to obtain

$$\pi = \left[\pi_a^2 : 2\pi_a\pi_b : \eta_{\mathsf{bb}}\pi_b^2 : 2\pi_a\pi_c : 2\eta_{\mathsf{bb}}\eta_{\mathsf{bc}}\pi_b\pi_c : \eta_{\mathsf{cc}}\eta_{\mathsf{bc}}^2\eta_{\mathsf{bb}}\pi_c^2\right], \tag{3.4}$$

where π_a, π_b and π_c are the functions of x given by (3.2).

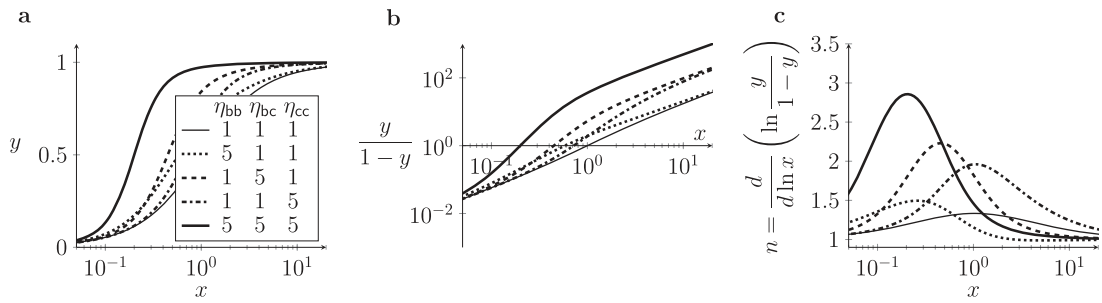

FIG. 4. (a) The fraction of occupied ligand binding sites (3.6) in the homodimer model (Fig. 3b) for different values of the allosteric parameters η_{bb}, η_{bc} and η_{cc}. (b,c) Hill plots show that interactions between the monomers may lead to cooperativity.

Equation (3.4) is significant. Without assuming independence, we have expressed the state probabilities of a receptor homodimer in terms of...

- the state probabilities of an isolated monomer (π_a, π_b and π_c, determined by κ_b, and κ_c) and
- the allosteric parameters η_{bb}, η_{bc} and η_{cc} that represent the possibility of conformational coupling.

In the absence of allosteric interactions, $\eta_i = 1$ and (3.4) simplifies as expected ($\pi_{a^2} = \pi_a^2, \pi_{ab} = 2\pi_a\pi_b$ etc.).

3.3 *Allosteric interactions influence receptor dimer binding curves*

Figure 4 illustrates the influence of allosteric parameters (i.e. conformational coupling between monomers) on the binding curve of a receptor dimer. Using the 6-state receptor dimer model discussed in the previous section (Fig. 3b), Fig. 4a plots the fraction of occupied ligand binding sites (four in the dimer, two for each monomer) as a function of ligand concentration x. The fraction of occupied sites is

$$y = \frac{1}{4}\pi_{ab} + \frac{1}{2}(\pi_{b^2} + \pi_{ac}) + \frac{3}{4}\pi_{bc} + \pi_{c^2}\,, \tag{3.5}$$

where π_{ab}, π_{b^2} etc., are given by (3.3)and (3.4). When the fraction of occupied ligand binding sites is written in terms of the monomer state probabilities and allosteric parameters, (3.5) becomes

$$y = \frac{1}{2}\pi_a\pi_b + \frac{1}{2}\eta_{bb}\pi_b^2 + \pi_a\pi_c + \frac{3}{2}\eta_{bc}\eta_{bb}\pi_b\pi_c + \eta_{cc}\eta_{bc}^2\eta_{bb}\pi_c^2\,, \tag{3.6}$$

where we have used $\pi_{b^2} = \eta_{bb}\pi_b^2$, $\pi_{bc} = 2\eta_{bc}\eta_{bb}\pi_b\pi_c$ etc., obtained by identifying (3.3) and (3.4). In this expression, π_a, π_b and π_c are given by (3.2).

The Hill plots in Fig. 4(b and c) show how the allosteric parameters (η_{bb}, η_{bc} and η_{cc}) that represent the interactions between the monomers may lead to cooperativity in the fraction of occupied binding sites. This example is reminiscent of a sequential (as opposed to concerted) model of cooperative oxygen binding in haemoglobin that accounts for the inequivalence of α and β subunits (Di Cera, 2005; Eaton *et al.*, 2007). In this interpretation, the original three-state model (3.1) is analogous to a $\alpha\beta$ haemoglobin dimer, and the allosteric parameter η_{bb} is the increase in affinity for the second binding event. The 6-state model represents a haemoglobin tetramer, in which η_{bc} and η_{cc} represent affinity changes resulting from interactions between $\alpha\beta$ dimers.

3.4 *A theory of allostery in oligomeric receptor models*

The remainder of this paper presents a general theory of allostery in oligomeric receptor models composed of any number of identical and indistinguishable monomers. In Section 4, we provide a construction of the state-transition diagram of receptor homodimers (and oligomers), for any given monomer topology. Section 5 calculates the number of thermodynamic constraints in an arbitrary receptor oligomers in terms of the monomer topology (i.e. without having to construct the state-transition graph of the oligomer). Sections 6–9 show how to enumerate the emergent allosteric interactions of receptor oligomers. In this way, the equilibrium state probabilities of a receptor oligomer may be understood in terms of the properties of an isolated monomer and allosteric parameters, each of which has a clear biophysical interpretation with respect to conformational coupling of the constituent monomers.

4. The state-transition diagram for a receptor oligomer is a reduced graph power

Let $G = (V, E)$ denote an undirected graph with v vertices and e edges. Formally, the vertex set is $V = \{a_1, a_2, \ldots, a_v\}$, but for readability we will often use the first v letters of the alphabet, $V = \{a, b, c, d, \ldots\}$. Each element of the set of edges, E, is an unordered pair of vertices. When we say that the graph G has the same structure (topology) as a receptor monomer of interest, we mean that the undirected edge (a_i, a_j) is an element of $E(G)$ precisely when there is a reversible transition between states a_i and a_j in the monomer state-transition diagram. For a monomer with v states and e transitions, G will have $v = |V|$ vertices and $e = |E|$ edges (using the common notation for the number of elements in a finite set). We assume G has no loops or multiple edges and is connected.

What graph corresponds to a receptor homomer composed of k identical subunits with topology given by G? The answer to this question is the kth reduced power of G (Hammack & Smith, 2017), denoted by $G^{(k)}$, which is formally defined as a product graph that is contracted using the symmetries of indistinguishable monomers (see Section S5 in the supplemental materials for mathematical details). For readers with no prior knowledge of product graphs, the state-transition graph of a receptor homo-oligomer can be constructed in three easy steps, as follows.

(1) For a receptor model of interest, construct an undirected graph with same topology. For example, an undirected graph $H = (V, E)$ corresponding to the ternary complex model (Fig. 1) has vertex set $V = \{a, b, c, d\}$ and edge set $E = \{(a, b), (a, c), (b, d), (c, d)\}$ (graph H in Fig. 5).

(2) Interpreting the vertex labels as variables, write their sum, raise this quantity to the kth power and expand. Each term of the resulting polynomial corresponds to a state of the receptor homo-oligomer. For a dimer composed of $k = 2$ indistinguishable ternary complex monomers, there are 10 distinguishable states

$$(a + b + c + d)^2 = a^2 + 2ab + 2ac + 2ad + b^2 + 2bc + 2bd + c^2 + 2cd + d^2 . \tag{4.1}$$

For a ternary complex tetramer, $k = 4$ and $(a+b+c+d)^4 = a^4 + a^3b + a^3c + \cdots + d^4$ gives 35 states. In general, the number of states in the receptor oligomer is given by v multi-choose k, i.e.

$$\left|V(G^{(k)})\right| = \left(\!\!\binom{v}{k}\!\!\right) = \binom{v + k - 1}{k} = \frac{(v + k - 1)!}{k!\ (v - 1)!} . \tag{4.2}$$

This is the number of ways k indistinguishable monomers can each be assigned to one of v states.

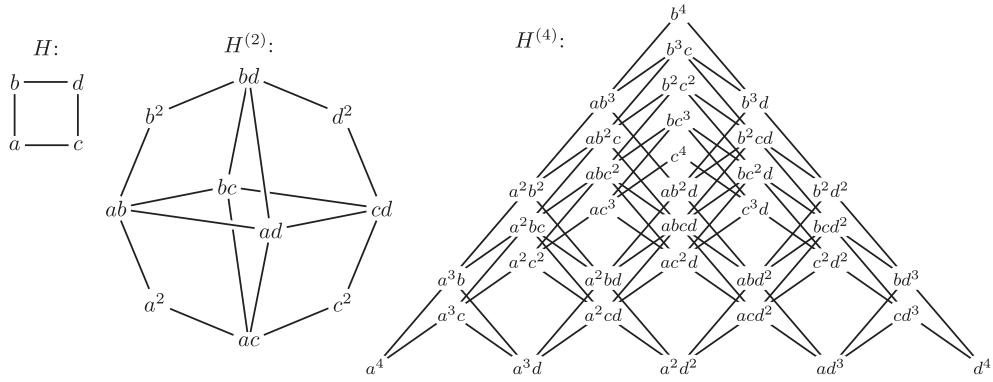

FIG. 5. Left: Undirected graph with topology of ternary complex model (Fig. 1). Middle: Topology of a homodimer composed of two identical and indistinguishable ternary complex monomers is given by the reduced graph power $H^{(2)}$. Right: Topology of a receptor oligomer composed of four identical ternary complex monomers is given by the reduced power $H^{(4)}$.

(3) For edges of the receptor oligomer state-transition graph, notice that if (a_i, a_j) is an edge of G (an allowed transition in the monomer), there is an edge between two states of $G^{(k)}$ (a transition in the oligomer) precisely when these states can be written as $a_i f_{k-1} = a_j f_{k-1}$ where $f_{k-1}(a_1, a_2, \ldots, a_v)$ is a monomial of degree $k-1$. The monomial f_{k-1} will be referred to as the *context* of the $a_i \rightleftharpoons a_j$ transition, i.e. the unchanged state of $k-1$ monomers when one monomer changes state from a_i to a_j or vice versa. Evidently, the number of edges of $G^{(k)}$ is

$$\left|E(G^{(k)})\right| = e\left(\!\!\binom{v}{k-1}\!\!\right) = e\binom{v+k-2}{k-1} = e\frac{(v+k-2)!}{(k-1)!\,(v-1)!}\,. \tag{4.3}$$

This is the product of number of edges of G, given by $e = |E(G)|$, and the number of contexts, which is the number of ways $k-1$ indistinguishable monomers can each be assigned to one of v states.

Figure 5 shows the reduced graph power $H^{(2)}$ that gives the topology of the state-transition diagram for a ternary complex homodimer. $H^{(2)}$ has $4\binom{4+2-2}{1} = 4\binom{4}{1} = 16$ edges. The edge (ab, bd) of $H^{(2)}$ corresponds to one monomer making an $a \rightleftharpoons d$ transition in the context of the other monomer occupying state b. Figure 5 also shows the graph $H^{(4)}$ for a receptor oligomer composed of four indistinguishable ternary complex monomers. $H^{(4)}$ has $4\binom{4+4-2}{3} = 4\binom{6}{3} = 80$ edges. The edge (b^2cd, bc^2d) of $H^{(4)}$ corresponds to one monomer of the receptor 4-mer making an $b \rightleftharpoons c$ transition in the context of bcd.

5. Thermodynamic constraints in receptor oligomers

The number of thermodynamic constraints in a receptor model is given by its Betti number, which is the dimension of the cycle space (sometimes called the nullity) of the state-transition graph (see Section S6 for a formal definition of the cycle space of a graph). For a graph G that is connected and has no loops or multiple edges, its Betti number is given by $\beta(G) = |E(G)| - |V(G)| + 1 = e - v + 1$. The number of free equilibrium parameters in the monomer model is the number of edges less the constraints $(e - \beta)$, which is equal to $v - 1$, the number of edges in a spanning tree of G.

How many thermodynamic constraints are present in a receptor oligomer obtained from G? Using (4.2) and (4.3), one finds that the Betti number of the reduced graph power $G^{(k)}$ is

$$\beta(G^{(k)}) = \left|E(G^{(k)})\right| - \left|V(G^{(k)})\right| + 1 = e\binom{v+k-2}{k-1} - \binom{v+k-1}{k} + 1\,. \tag{5.1}$$

The number of free equilibrium parameters in a receptor oligomer model is

$$\left|E(G^{(k)})\right| - \beta(G^{(k)}) = \left|V(G^{(k)})\right| - 1 = \binom{v+k-1}{k} - 1\,, \tag{5.2}$$

which is the number of edges in a spanning tree of the reduced graph power $G^{(k)}$. For example, the ternary complex homodimer, shown as $H^{(2)}$ in Fig. 5, has $\beta(H^{(2)}) = 16 - 10 + 1 = 7$ thermodynamic constraints and 9 free parameters. The ternary complex tetramer, shown as $H^{(4)}$ in Fig. 5, has $\beta(H^{(4)}) = 80 - 35 + 1 = 46$ thermodynamic constraints and 34 free equilibrium parameters. The next section discusses the biophysically meaningful assignment of these equilibrium parameters.

6. Equilibrium parameters in receptor monomers and oligomers

Our goal is to assign equilibrium parameters to a receptor oligomer in a manner that clarifies the possible interactions between monomers (i.e. conformational coupling). We begin by introducing a convention for assignment of equilibrium parameters to the edges of G, the state-transition graph of the monomer, whose vertex set is $V(G) = \{a_1, a_2, \ldots, a_v\}$. To accomplish this, we first construct a rooted spanning tree of G with root a_1 and indexing that respects a breadth-first traversal (denoted T_G or just T). Any edge of T is uniquely determined by its endpoint a_j that is furthest from the root. For each $2 \leqslant i \leqslant v$, let e_j be the edge of T that has endpoints a_i and a_j, with a_j further from the root than a_i. For each edge of T, we have $\mathsf{e}_i = (a_i^-, a_i)$, where a_i^- is the predecessor of a_i. For each edge e_i of T, there is a free equilibrium constant that will be denoted by κ_{e_i}.

For the ternary complex monomer introduced in Fig. 1, denoted H in Fig. 5, an example spanning tree (T_H) is shown below left.

The edges of T_H are $\mathsf{b} = (a, b)$, $\mathsf{c} = (a, c)$, $\mathsf{d} = (b, d)$ and the predecessors are $b^- = a$, $c^- = a$, and $d^- = b$. The root vertex a has no predecessor. For convenience, we have chosen T_H so each directed edges (b, c and d) points backwards (reactant $\leftarrow$ product). The free equilibrium constants are denoted κ_{b}, κ_{c} and κ_{d} (shown above right). The constrained equilibrium constant is $\kappa_{\mathsf{x}} = \kappa_{\mathsf{b}}\kappa_{\mathsf{d}}/\kappa_{\mathsf{c}}$. In the notation of Fig. 1, $\kappa_{\mathsf{b}} = K_L[L]$, $\kappa_{\mathsf{c}} = K_G[G]$ and $\kappa_{\mathsf{d}} = \gamma K_G[G]$ and $\kappa_{\mathsf{x}} = \gamma K_L[L]$.

We may now formally assign equilibrium parameters to the edges of the receptor oligomer state-transition graph $G^{(k)}$. Because T_G is a spanning tree of G, the reduced power of this spanning tree, denoted $T_G^{(k)}$, is a subgraph of $G^{(k)}$ that spans $G^{(k)}$. Although $T_G^{(k)}$ spans $G^{(k)}$, it is not a tree. In fact, $T_G^{(k)}$

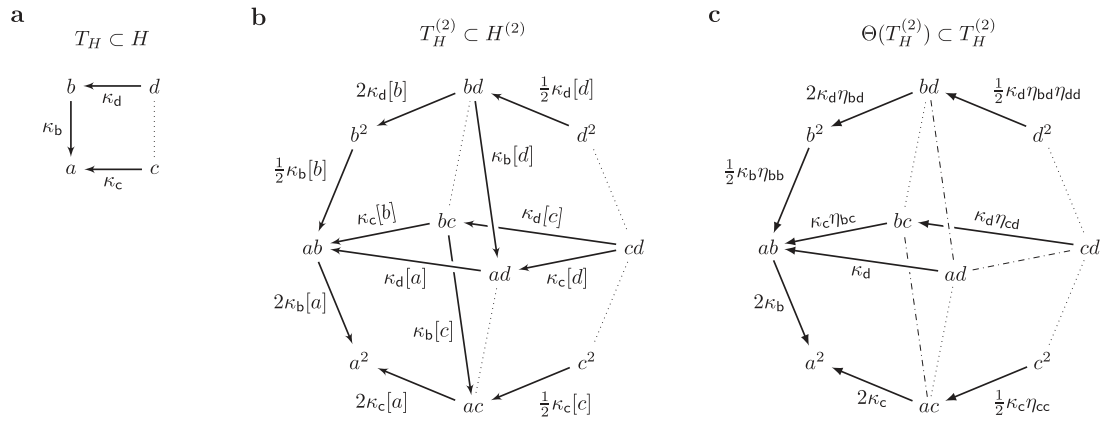

FIG. 6. (a,b) Because T_H is a spanning tree of H, the reduced graph power of T_H, denoted $T_H^{(2)}$, spans $H^{(2)}$. However, $T_H^{(2)}$ has three Cartesian squares and is not a tree. (c) $\Theta(T_H^{(2)})$ is a spanning tree obtained from $T_H^{(2)}$ by eliminating three edges (shown dash-dotted), one from each Cartesian square. The parameters labelling edges of $T_H^{(2)}$ in (b) are transition-context pairs, e.g., $\kappa_{\mathsf{d}}[b]$ denotes the equilibrium constant for reaction $\mathsf{d} = (b,d)$ in one ternary complex monomer when the other monomer is in state b. In (c), the nine free parameters of ternary complex homodimer are specified as three equilibrium constants inherited from the monomer (κ_i for $i \in \{\mathsf{b},\mathsf{c},\mathsf{d}\}$) and six allosteric parameters (η_{ij} for $i,j \in \{\mathsf{b},\mathsf{c},\mathsf{d}\}$ and $i \leqslant j$).

will include $\binom{v-1}{2}$ Cartesian squares (a special type of 4-cycle), one for each distinct pair of edges in T_G (see Section S6). However, a spanning tree of $G^{(k)}$, denoted by $\Theta(T_G^{(k)})$, can always be constructed by eliminating edges of $T_G^{(k)}$ in such a way that each successive edge removed breaks a Cartesian square. The edges of the spanning tree $\Theta(T_G^{(k)}) \subset G^{(k)}$ will be transition-context pairs involving an edge of T_G (the transition), denoted $\mathsf{e}_i = (a_i^-, a_i)$, and a monomial $f_{k-1}(a_1, a_2, \ldots, a_v)$ of degree $k-1$ (the context). The equilibrium constants labelling the edges of $\Theta(T_G^{(k)})$ are formally denoted as $\kappa_{\mathsf{e}_i}[f_{k-1}]$ where $2 \leqslant i \leqslant v$. The next paragraphs illustrate the pruning of $T_G^{(k)}$ that leads to the spanning tree $\Theta(T_G^{(k)})$ using our two running examples, the ternary complex dimer and tetramer.

Figure 6b shows $T_H^{(2)}$ where T_H is the spanning tree of the ternary complex model shown as H in Fig. 6a. The $\binom{v-1}{2} = \binom{3}{2} = 3$ Cartesian squares are $a^2 + ac + ab + bc$, $ab + ad + b^2 + bd$ and $ab + bd + bc + cd$. Using this notation, the equilibrium parameters for the spanning tree $\Theta(T_H^{(2)})$ are $\kappa_{\mathsf{b}}[a]$ for the edge (a^2, ab), $\kappa_{\mathsf{b}}[b]$ for (ab, b^2), $\kappa_{\mathsf{d}}[c]$ for (bc, cd) and so on (see Fig. 6b). Figure 6c shows the spanning tree $\Theta(T_H^{(2)})$ that is obtained by eliminating one edge from each Cartesian square in $T_H^{(2)}$ (the three eliminated edges are shown dash-dotted).

The arrows of Fig. 7 show a spanning tree $\Theta(T_H^{(4)})$ for the ternary complex tetramer $H^{(4)}$ that is constructed in a similar fashion. $\Theta(T_H^{(4)})$ has $\binom{v+k-1}{k} - 1 = \binom{7}{4} - 1 = 34$ edges (shown solid). The reduced graph product $T_H^{(4)}$ has $(v-1)\binom{v+k-2}{k-1} = 3\binom{6}{3} = 60$ edges (solid and dash-dotted but not dotted). Figure 7 also shows the equilibrium constants for several transitions that are shown: $\kappa_{\mathsf{b}}[a^3]$ for the edge (a^4, a^3b) representing an $a \rightleftharpoons b$ transition in the context of a^3; $\kappa_{\mathsf{b}}[a^2b]$ for (a^3b, a^2b^2) representing an $a \rightleftharpoons b$ transition in the context of a^2b; $\kappa_{\mathsf{d}}[b^3]$ for (b^4, b^3d) representing an $b \rightleftharpoons d$ transition in the context of b^3; $\kappa_{\mathsf{d}}[a^2b]$ for (abd^2, ad^3) representing an $b \rightleftharpoons d$ transition in the context of a^2b. Note that

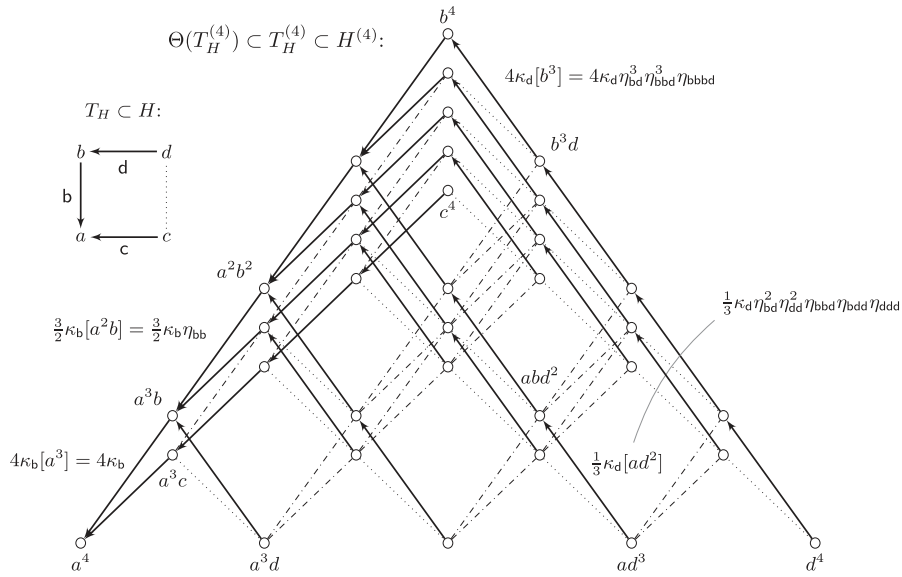

FIG. 7. The graph T_H is a rooted spanning tree of H. The graph $T_H^{(4)}$ is the subgraph of $H^{(4)}$ shown solid and dash-dotted (but not dotted). The solid arrows are $\Theta(T_H^{(4)})$, the subgraph of $T_H^{(4)}$ that is the distinguished spanning tree of $H^{(4)}$. Several edges of $\Theta(T_H^{(4)})$ are labelled as transition-context pairs.

there are $\binom{v-1}{2}\binom{k+v-3}{k-2} = \binom{3}{2}\binom{5}{2} = 30$ Cartesian squares in the reduced graph product $T_H^{(4)}$, but not all of these are independent (see Section S6). A total of 26 edges of $T_H^{(4)}$ are eliminated to obtain the spanning tree $\Theta(T_H^{(4)})$ (the eliminated edges are shown dash-dotted).

7. Enumerating allosteric interactions in receptor dimers

How should the free parameters for a receptor oligomer be specified to illuminate the possible allosteric interactions among monomers? Because the spanning tree T_G has $e = v - 1$ edges, we may define $(e+1)e/2 = v(v-1)/2$ independent 2-way allosteric parameters (the number of ways 2 edges can be chosen from the spanning tree with replacement). For a dimer ($k = 2$), these 2-way parameters are

$$\eta_{\mathsf{e}_i\mathsf{e}_j} := \frac{\kappa_{\mathsf{e}_i}[a_j]}{\kappa_{\mathsf{e}_i}[a_j^-]} = \frac{\kappa_{\mathsf{e}_j}[a_i]}{\kappa_{\mathsf{e}_j}[a_i^-]}, \tag{7.1}$$

where $2 \leqslant i \leqslant j \leqslant v$. For example, the spanning tree T_H of the ternary complex monomer has three edges (b, c, d). Thus, there are $4 \cdot 3/2 = 6$ allosteric parameters for the dimer,

$$\eta_{\mathsf{bb}} = \kappa_{\mathsf{b}}[b]/\kappa_{\mathsf{b}}[a] \tag{7.2}$$

$$\eta_{\mathsf{bc}} = \kappa_{\mathsf{b}}[c]/\kappa_{\mathsf{b}}[a] = \kappa_{\mathsf{c}}[b]/\kappa_{\mathsf{c}}[a] \tag{7.3}$$

$$\eta_{\mathsf{bd}} = \kappa_{\mathsf{b}}[d]/\kappa_{\mathsf{b}}[b] = \kappa_{\mathsf{d}}[b]/\kappa_{\mathsf{d}}[a] \tag{7.4}$$

$$\eta_{\mathsf{cc}} = \kappa_{\mathsf{c}}[c]/\kappa_{\mathsf{c}}[a] \tag{7.5}$$

$$\eta_{\mathsf{cd}} = \kappa_{\mathsf{c}}[d]/\kappa_{\mathsf{c}}[b] = \kappa_{\mathsf{d}}[c]/\kappa_{\mathsf{d}}[a] \tag{7.6}$$

$$\eta_{\mathsf{dd}} = \kappa_{\mathsf{d}}[d]/\kappa_{\mathsf{d}}[b]\,. \tag{7.7}$$

Using the 2-way allosteric parameters defined above and the equilibrium parameters inherited from the monomer model ($\kappa_{\mathsf{b}}[a] = \kappa_{\mathsf{b}}$, $\kappa_{\mathsf{c}}[a] = \kappa_{\mathsf{c}}$, $\kappa_{\mathsf{d}}[a] = \kappa_{\mathsf{d}}$ because a is the root of T_H), we are able to specify the equilibrium constants for each edge of $\Theta(T_H^{(2)})$ in a manner that illuminates the possibility of conformational coupling. For example, the parameter on edge (ab, b^2) is formally $\kappa_{\mathsf{b}}[b]$ because this edge is a $\mathsf{b} = (a, b)$ transition in the context of b. Using (7.2), we have $\kappa_{\mathsf{b}}[b] = \kappa_{\mathsf{b}}[a]\eta_{\mathsf{bb}} = \kappa_{\mathsf{b}}\eta_{\mathsf{bb}}$. The edge (bd, d^2) is a $\mathsf{d} = (b, d)$ transition in the context of d. Using both (7.2) and (7.7), we see that this equilibrium constant is $\kappa_{\mathsf{d}}[d] = \kappa_{\mathsf{d}}[b]\eta_{\mathsf{dd}} = \kappa_{\mathsf{d}}\eta_{\mathsf{bd}}\eta_{\mathsf{dd}}$. Repeating this process for all 10 states yields the specification of allosteric parameters in the ternary complex homodimer shown in Fig. 6b. The corresponding binding curve [$\pi_{a^2} : \pi_{ab} : \pi_{ac} : \pi_{ad} : \pi_{b^2} : \pi_{bc} : \pi_{bd} : \pi_{c^2} : \pi_{cd} : \pi_{d^2}$] is

$$\left[\, 1 : 2\kappa_{\mathsf{b}} : \kappa_{\mathsf{b}}^2\eta_{\mathsf{bb}} : 2\kappa_{\mathsf{c}} : 2\kappa_{\mathsf{b}}\kappa_{\mathsf{c}}\eta_{\mathsf{bc}} : \kappa_{\mathsf{c}}^2\eta_{\mathsf{cc}} : 2\kappa_{\mathsf{b}}\kappa_{\mathsf{d}} : 2\kappa_{\mathsf{b}}^2\kappa_{\mathsf{d}}\eta_{\mathsf{bd}}\eta_{\mathsf{bb}} : 2\kappa_{\mathsf{b}}\kappa_{\mathsf{c}}\kappa_{\mathsf{d}}\eta_{\mathsf{bc}}\eta_{\mathsf{cd}} : \kappa_{\mathsf{b}}^2\kappa_{\mathsf{d}}^2\eta_{\mathsf{bb}}\eta_{\mathsf{bd}}^2\eta_{\mathsf{dd}} \,\right]. \tag{7.8}$$

Dividing (7.8) by $(1 + \kappa_{\mathsf{b}} + \kappa_{\mathsf{c}} + \kappa_{\mathsf{b}}\kappa_{\mathsf{d}})^2$ gives

$$\left[\pi_a^2 : 2\pi_a\pi_b : \pi_b^2\eta_{\mathsf{bb}} : 2\pi_a\pi_c : 2\pi_b\pi_c\eta_{\mathsf{bc}} : \pi_c^2\eta_{\mathsf{cc}} : 2\pi_a\pi_d : 2\pi_b\pi_d\eta_{\mathsf{bd}}\eta_{\mathsf{bb}} : 2\pi_c\pi_d\eta_{\mathsf{bc}}\eta_{\mathsf{cd}} : \pi_d^2\eta_{\mathsf{bb}}\eta_{\mathsf{bd}}^2\eta_{\mathsf{dd}}\right], \tag{7.9}$$

where $[\pi_a : \pi_b : \pi_c : \pi_d] = [1 : \kappa_{\mathsf{b}} : \kappa_{\mathsf{c}} : \kappa_{\mathsf{b}}\kappa_{\mathsf{d}}]$. Without assuming independence of receptor monomers, we have expressed the equilibrium occupancy measure of the ternary complex homodimer in terms of the properties of an isolated monomer (π_a, π_b etc.) and allosteric parameters (η_{bb}, η_{bc} etc.). Some readers may prefer Fig. 8, which is Fig. 6c recast in the biophysical notation of Fig. 1.

8. Enumerating allosteric interactions in higher-order receptor oligomers

For receptor oligomers with $k > 2$, the 2-way allosteric parameters take the form

$$\eta_{\mathsf{e}_i\mathsf{e}_j}[f_{k-2}] := \frac{\kappa_{\mathsf{e}_i}[a_j f_{k-2}]}{\kappa_{\mathsf{e}_i}[a_j^- f_{k-2}]} = \frac{\kappa_{\mathsf{e}_j}[a_i f_{k-2}]}{\kappa_{\mathsf{e}_j}[a_i^- f_{k-2}]}\,,$$

where $2 \leqslant i \leqslant j \leqslant v$ and $f_{k-2}(a_1, a_2, \ldots, a_v)$ is a monomial of degree $k - 2$. This is a generalization of (7.1) because $f_{k-2} = 1$ when $k = 2$. When $k > 2$, there are also multiway allosteric interactions that must be considered. For example, the 3-way allosteric parameters are

$$\eta_{\mathsf{e}_i\mathsf{e}_j\mathsf{e}_h}[f_{k-3}] := \frac{\eta_{\mathsf{e}_i\mathsf{e}_j}[a_h f_{k-3}]}{\eta_{\mathsf{e}_i\mathsf{e}_j}[a_h^- f_{k-3}]} = \frac{\eta_{\mathsf{e}_i\mathsf{e}_h}[a_j f_{k-3}]}{\eta_{\mathsf{e}_i\mathsf{e}_h}[a_j^- f_{k-3}]} = \frac{\eta_{\mathsf{e}_j\mathsf{e}_h}[a_i f_{k-3}]}{\eta_{\mathsf{e}_j\mathsf{e}_h}[a_i^- f_{k-3}]}, \tag{8.1}$$

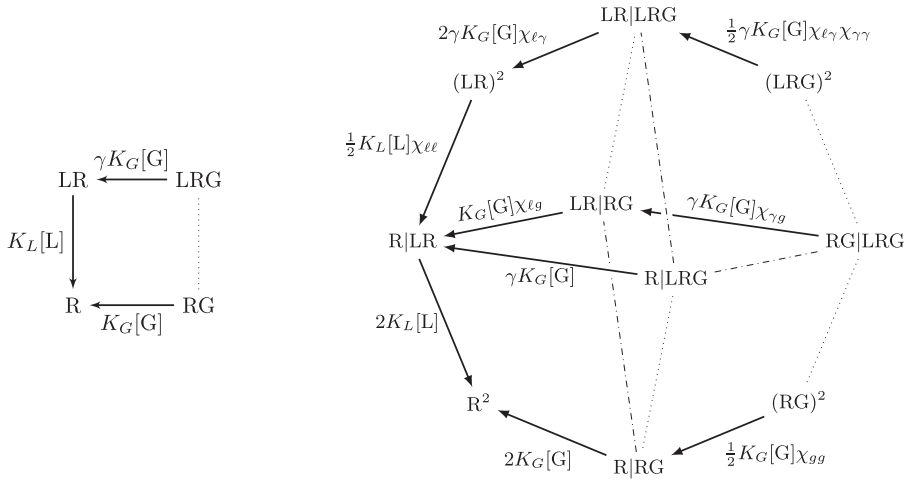

FIG. 8. Left: Spanning tree of the ternary complex model (cf. Fig. 1). Right: Specification of allosteric parameters in the ternary complex dimer given by Fig. 6c with the replacements $a \to R$, $b \to$ LR, $c \to$ RG, $d \to$ LRG, $\eta_{\mathsf{bb}} \to \chi_{\ell\ell}$, $\eta_{\mathsf{bc}} \to \chi_{\ell g}$, $\eta_{\mathsf{bd}} \to \chi_{\ell\gamma}$, $\eta_{\mathsf{cc}} \to \chi_{gg}$, $\eta_{\mathsf{cd}} \to \chi_{g\gamma}$, $\eta_{\mathsf{dd}} \to \chi_{\gamma\gamma}$ where ℓ, g and γ stand for the transitions R $\rightleftharpoons$ LR, R $\rightleftharpoons$ RG and LR $\rightleftharpoons$ LRG, respectively.

where $2 \leqslant i \leqslant j \leqslant h \leqslant v$ and $f_{k-3}(a_1, a_2, \ldots, a_v)$ is a monomial of degree $k-3$ ($f_{k-3} = 1$ when $k = 3$). The equalities in (8.1) may be confirmed by expanding the definition, for example,

$$\frac{\eta_{\mathsf{e}_i\mathsf{e}_j}[a_h f_{k-3}]}{\eta_{\mathsf{e}_i\mathsf{e}_j}[a_h^- f_{k-3}]} = \frac{\kappa_{\mathsf{e}_i}[a_j a_h f_{k-3}]/\kappa_{\mathsf{e}_i}[a_j^- a_h f_{k-3}]}{\kappa_{\mathsf{e}_i}[a_j a_h^- f_{k-3}]/\kappa_{\mathsf{e}_i}[a_j^- a_h^- f_{k-3}]}$$
$$= \frac{\kappa_{\mathsf{e}_i}[a_h a_j f_{k-3}]/\kappa_{\mathsf{e}_i}[a_h^- a_j f_{k-3}]}{\kappa_{\mathsf{e}_i}[a_h a_j^- f_{k-3}]/\kappa_{\mathsf{e}_i}[a_h^- a_j^- f_{k-3}]} = \frac{\eta_{\mathsf{e}_i\mathsf{e}_h}[a_j f_{k-3}]}{\eta_{\mathsf{e}_i\mathsf{e}_h}[a_j^- f_{k-3}]}.$$

In general, for $2 \leqslant n \leqslant k$, n-way allosteric parameters are defined as

$$\eta_{e_{i_1}e_{i_2}\cdots e_{i_n}}[f_{k-n}] := \frac{\eta_{e_{i_1}e_{i_2}\cdots e_{i_{\ell-1}}e_{i_{\ell+1}}\cdots e_{i_n}}[a_{i_\ell} f_{k-n}]}{\eta_{e_{i_1}e_{i_2}\cdots e_{i_{\ell-1}}e_{i_{\ell+1}}\cdots e_{i_n}}[a_{i_\ell}^- f_{k-n}]}, \quad 1 \leqslant \ell \leqslant n,$$

where $2 \leqslant i_1 \leqslant i_2 \leqslant \cdots \leqslant i_n \leqslant v$ and $f_{k-n}(a_1, a_2, \ldots, a_v)$ is a monomial of degree $k-n$. Note that the n-way allosteric parameter $\eta_{e_{i_1}e_{i_2}\cdots e_{i_n}}$ has m equivalent definitions where m is the number of distinct subscripts.

For a monomer topology given by G, the spanning tree T_G has $v-1$ edges. A receptor oligomer composed of k monomers has $\left(\!\binom{v-1}{n}\!\right) = \binom{v+n-2}{n}$ n-way allosteric parameters for $2 \leqslant n \leqslant k$, which is the number of ways that n of the $v-1$ edges can be chosen with replacement. For example, the spanning tree $\Theta(T_H^{(4)})$ of the ternary complex 4-mer has $\binom{4}{2} = 6$ 2-way, $\binom{5}{3} = 10$ 3-way and $\binom{6}{4} = 15$ 4-way

parameters. Some of these are

$$\begin{aligned}
\eta_{\mathsf{bbb}} &= \eta_{\mathsf{bb}}[b]/\eta_{\mathsf{bb}}[a] \\
\eta_{\mathsf{ccd}} &= \eta_{\mathsf{cc}}[d]/\eta_{\mathsf{cc}}[b] = \eta_{\mathsf{cd}}[c]/\eta_{\mathsf{cd}}[a] \\
\eta_{\mathsf{bcd}} &= \eta_{\mathsf{bc}}[d]/\eta_{\mathsf{bc}}[b] = \eta_{\mathsf{bd}}[c]/\eta_{\mathsf{bd}}[a] = \eta_{\mathsf{cd}}[b]/\eta_{\mathsf{cd}}[a] \\
\eta_{\mathsf{bbcd}} &= \eta_{\mathsf{bbc}}[d]/\eta_{\mathsf{bbc}}[b] = \eta_{\mathsf{bbd}}[c]/\eta_{\mathsf{bbd}}[a] = \eta_{\mathsf{bcd}}[b]/\eta_{\mathsf{bcd}}[a] \\
\eta_{\mathsf{ccdd}} &= \eta_{\mathsf{ccd}}[d]/\eta_{\mathsf{ccd}}[b] = \eta_{\mathsf{cdd}}[c]/\eta_{\mathsf{cdd}}[a] \\
\eta_{\mathsf{dddd}} &= \eta_{\mathsf{ddd}}[d]/\eta_{\mathsf{ddd}}[b].
\end{aligned}$$

Specifying allosteric interactions in this fashion introduces the number of parameters required to specify a receptor oligomer model, which is the number of edges in spanning tree $\Theta(T_G^{(k)})$, i.e. $\left(\!\binom{v}{k}\!\right) - 1 = \binom{v+k-1}{k} - 1$ where $v = |V(G)|$. To see this, note that the number of n-way allosteric interactions involving the $v-1$ edges of the spanning tree T_G is $\left(\!\binom{v-1}{n}\!\right)$. When $n = 1$, this is $\left(\!\binom{v-1}{1}\!\right) = v - 1$, i.e. the number of free parameters in the monomer. When these are supplemented with allosteric parameters for 2-way through k-way interactions, the total number of parameters obtained is

$$\begin{aligned}
v - 1 + \sum_{n=2}^{k} \left(\!\binom{v-1}{n}\!\right) = \sum_{n=1}^{k} \left(\!\binom{v-1}{n}\!\right) \quad &= -1 + \sum_{n=0}^{k} \left(\!\binom{v-1}{n}\!\right) \\
&= -1 + \sum_{n=0}^{k} \binom{v+n-2}{n} = -1 + \binom{v+k-1}{k},
\end{aligned}$$

which is the number of edges in the spanning tree $\Theta(T_G^{(k)})$.

9. Token method for specifying allosteric parameters

For receptor dimers with state-transition diagram $G^{(2)}$, the allosteric factors that were discussed in the previous sections may be enumerated using a natural 'token' representation of receptor oligomer states. To begin, draw the tree T_G that spans the state-transition graph G of the monomer. For any given state of the oligomer, put (indistinguishable) tokens in the positions associated with the monomer states. For example, the token graphs associated to states bd and d^2 in the ternary complex dimer, $H^{(2)}$, are

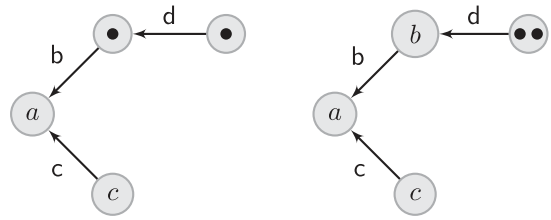

To calculate allosteric factor for state bd, consider the path of each token to the root (the vertex a). These paths yield b for the first token and $\mathsf{b}+\mathsf{d}$ for the second token. Because the product is $\mathsf{b}(\mathsf{b}+\mathsf{d}) = \mathsf{b}^2+\mathsf{bd}$,

TABLE 1 *Worksheet for the token method for enumerating allosteric parameters in the case of the ternary complex dimer. Compare (7.9) and Fig. 6c.*

State	Token 1	Token 2	Sum	1-Way	Product	2-Way
a^2	0	0	0	0	0	-
ab	0	b	b	κ_b	0	-
b^2	b	b	$2\mathsf{b}$	κ_b^2	b^2	η_{bb}
ac	0	$\mathsf{b}+\mathsf{c}$	$\mathsf{b}+\mathsf{c}$	$\kappa_\mathsf{b}\kappa_\mathsf{c}$	0	-
bc	b	$\mathsf{b}+\mathsf{c}$	$2\mathsf{b}+\mathsf{c}$	$\kappa_\mathsf{b}^2\kappa_\mathsf{c}$	$\mathsf{b}^2+\mathsf{bc}$	$\eta_{\mathsf{bb}}\eta_{\mathsf{bc}}$
c^2	$\mathsf{b}+\mathsf{c}$	$\mathsf{b}+\mathsf{c}$	$2\mathsf{b}+2\mathsf{c}$	$\kappa_\mathsf{b}^2\kappa_\mathsf{c}^2$	$\mathsf{b}^2+2\mathsf{bc}+\mathsf{c}^2$	$\eta_{\mathsf{bb}}\eta_{\mathsf{bc}}^2\eta_{\mathsf{cc}}$
ad	0	d	d	κ_d	0	-
bd	b	d	$\mathsf{b}+\mathsf{d}$	$\kappa_\mathsf{b}\kappa_\mathsf{d}$	bd	η_{bd}
cd	$\mathsf{b}+\mathsf{c}$	d	$\mathsf{b}+\mathsf{c}+\mathsf{d}$	$\kappa_\mathsf{b}\kappa_\mathsf{c}\kappa_\mathsf{d}$	$\mathsf{bd}+\mathsf{cd}$	$\eta_{\mathsf{bd}}\eta_{\mathsf{cd}}$
d^2	d	d	$2\mathsf{d}$	κ_d^2	d^2	η_{dd}

the allosteric factor in the term $\pi_b\pi_d$ in (7.9) is $\eta_{\mathsf{bb}}\eta_{\mathsf{bd}}$. For state d^2, the path to root for both tokens is $b+d$ and the product is $(\mathsf{b}+\mathsf{d})^2=\mathsf{b}^2+2\mathsf{bd}+\mathsf{d}^2$; thus, the allosteric factor for π_d^2 is $\eta_{\mathsf{bb}}\eta_{\mathsf{bd}}^2\eta_{\mathsf{dd}}$. Table 1 shows the complete list of allosteric factors for the ternary complex dimer, $H^{(2)}$. Figure 6c shows the corresponding labelled spanning tree $\Theta(T_H^{(2)})$. The relative probability of any receptor dimer state (a^2, ab, $\ldots d^2$) can be read off this spanning tree. For example, the relative probability of state d^2 is found, using Fig. 6c, as the product of labels on the path from d^2 to the root ($a^2 \leftarrow ab \leftarrow \mathsf{b}^2 \leftarrow bd \leftarrow \mathsf{d}^2$). This product is $2\kappa_\mathsf{b}\cdot\frac{1}{2}\kappa_\mathsf{b}\eta_{\mathsf{bb}}\cdot 2\kappa_\mathsf{d}\eta_{\mathsf{bd}}\cdot\frac{1}{2}\kappa_\mathsf{d}\eta_{\mathsf{bd}}\eta_{\mathsf{dd}}=\kappa_\mathsf{b}^2\kappa_\mathsf{d}^2\eta_{\mathsf{bb}}\eta_{\mathsf{bd}}^2\eta_{\mathsf{dd}}$ (7.8). Dividing by $(1+\kappa_\mathsf{b}+\kappa_\mathsf{c}+\kappa_\mathsf{b}\kappa_\mathsf{d})^2$ gives $\pi_d^2\eta_{\mathsf{bb}}\eta_{\mathsf{bd}}^2\eta_{\mathsf{dd}}$ (7.9).

The token method for a receptor k-mer where $k>2$ is more complicated than the special case of a receptor dimer where $k=2$. For a receptor k-mer, we may assume $p_1\leqslant p_2\leqslant\cdots\leqslant p_k$ where p_ℓ is the place of the ℓth token. Recall that $e_\ell=(a_\ell^-,a_\ell)$ and define $h(a_\ell)$ recursively,

$$h(a_\ell)=\begin{cases}0 & \text{for } a_\ell=a_1\\ e_\ell+h(a_\ell^-) & \text{otherwise.}\end{cases}\tag{9.1}$$

The n-way interactions are enumerated by the elementary symmetric polynomials in $h_1,h_2,\ldots,h_k$, namely,

$$\varepsilon_n(h_1,h_2,\ldots,h_k):=\sum_{1\leqslant i_1<i_2<\cdots<i_n\leqslant k}h_{i_1}h_{i_2}\cdots h_{i_n}.\tag{9.2}$$

For example, the token graphs associated to states bcd^2 and ac^2d in the ternary complex tetramer, shown in Fig. 5 as $H^{(4)}$, are

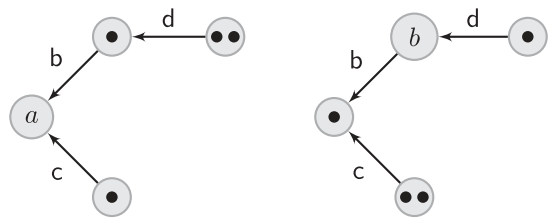

The 2-, 3- and 4-way interactions are (9.2)

$$\begin{aligned}
&\text{2-way}: h_1h_2 + h_1h_3 + h_1h_4 + h_2h_3 + h_2h_4 + h_3h_4\\
&\text{3-way}: h_1h_2h_3 + h_1h_2h_4 + h_1h_3h_4 + h_2h_3h_4\\
&\text{4-way}: h_1h_2h_3h_4
\end{aligned}$$

where (9.1)

$$\begin{aligned}
&bcd^2: h_1 = \mathsf{b} \quad h_2 = \mathsf{c} \quad h_3 = \mathsf{b}+\mathsf{d} \quad h_4 = \mathsf{b}+\mathsf{d}\\
&ac^2d: h_1 = 0 \quad h_2 = \mathsf{c} \quad h_3 = \mathsf{c} \quad h_4 = \mathsf{b}+\mathsf{d}.
\end{aligned}$$

For state bcd^2,

$$\begin{aligned}
\text{2-way}&: \mathsf{bc} + 2\mathsf{b}(\mathsf{b}+\mathsf{d}) + 2\mathsf{c}(\mathsf{b}+\mathsf{d}) + (\mathsf{b}+\mathsf{d})^2\\
&= 3\mathsf{b}^2 + 4\mathsf{bd} + 3\mathsf{bc} + \mathsf{d}^2 + 2\mathsf{cd}\\
\text{3-way}&: 2\mathsf{bc}(\mathsf{b}+\mathsf{d}) + \mathsf{b}(\mathsf{b}+\mathsf{d})^2 + \mathsf{c}(\mathsf{b}+\mathsf{d})^2\\
&= \mathsf{b}^3 + 2\mathsf{b}^2\mathsf{d} + 3\mathsf{b}^2\mathsf{c} + \mathsf{bd}^2 + 4\mathsf{bcd} + \mathsf{cd}^2\\
\text{4-way}&: \mathsf{bc}(\mathsf{b}+\mathsf{d})^2 = \mathsf{b}^3\mathsf{c} + 2\mathsf{b}^2\mathsf{cd} + \mathsf{bcd}^2.
\end{aligned}$$

Thus, the $\pi_b\pi_c\pi_d^2$ term, which has combinatorial coefficient $(1,1,2)! = 4!/(0!\,1!\,1!\,2!) = 12$, has allosteric factors

$$\underbrace{\eta_{\mathsf{bb}}^3\eta_{\mathsf{bd}}^4\eta_{\mathsf{bc}}^3\eta_{\mathsf{dd}}\eta_{\mathsf{cd}}^2}_{\text{2 way}}\ \underbrace{\eta_{\mathsf{bbb}}\eta_{\mathsf{bbd}}^2\eta_{\mathsf{bbc}}^3\eta_{\mathsf{bdd}}\eta_{\mathsf{bcd}}^4\eta_{\mathsf{cdd}}}_{\text{3 way}}\ \underbrace{\eta_{\mathsf{bbbc}}\eta_{\mathsf{bbcd}}^2\eta_{\mathsf{bcdd}}}_{\text{4 way}}.$$

For state ac^2d, a similar calculation gives

$$12\,\pi_a\pi_c^2\pi_d\,\eta_{\mathsf{bc}}^2\eta_{\mathsf{cc}}\eta_{\mathsf{cd}}^2\,\eta_{\mathsf{bcc}}\eta_{\mathsf{ccd}}.$$

Section S3.2 of the supporting material gives the complete result, obtained through a symbolic calculation of (9.1) and (9.2).

To find the allosteric factors associated to a given edge of the spanning tree $\Theta(T_H^{(4)})$, one may compare combinatorial coefficients and allosteric factors associated to state and its predecessor (both adjacent to the edge of interest). For example, the edge (abd^2, ad^3) represents the $b \rightleftharpoons d$ transition in the context of ad^2. This edge has the equilibrium constant $\frac{1}{3}\kappa_{\mathsf{d}}[ad^2]$ where the coefficient $1/3$ is the ratio of $(1,3)! = 4$ for ad^3 and $(1,1,2)! = 12$ for abd^2. Evaluating (9.2) gives $6\mathsf{bd} + 3\mathsf{bd}^2 + 3\mathsf{b}^2\mathsf{d} + 3\mathsf{b}^2 + \mathsf{b}^3 + 3\mathsf{d}^2 + \mathsf{d}^3$ for ad^3 and $4\mathsf{bd} + \mathsf{bd}^2 + 2\mathsf{b}^2\mathsf{d} + 3\mathsf{b}^2 + \mathsf{b}^3 + \mathsf{d}^2$ for abd^2. Because the difference is $2\mathsf{bd} + 2\mathsf{d}^2 + \mathsf{b}^2\mathsf{d} + 2\mathsf{bd}^2 + \mathsf{d}^3$, we conclude that $\frac{1}{3}\kappa_{\mathsf{d}}[ad^2] = \frac{1}{3}\kappa_{\mathsf{d}}\eta_{\mathsf{bd}}^2\eta_{\mathsf{dd}}^2\eta_{\mathsf{bbd}}\eta_{\mathsf{bdd}}^2\eta_{\mathsf{ddd}}$ (see Fig. 7).

Alternatively, one may calculate the allosteric factors associated to process d occurring in the context of ad^2 in the following, more direct fashion. The token graph associated to the context ad^2 involves the

following placement of 3 tokens,

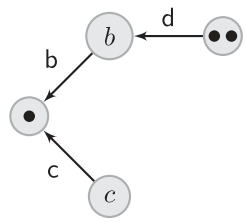

Reading this token graph we find $h_1 = 0$ and $h_2 = h_3 = \mathsf{b} + \mathsf{d}$. Substituting these values in (9.2) gives a polynomial associated to the context ad^2, namely,

$$\underbrace{h_1 + h_2 + h_3}_{1\text{ way}} + \underbrace{h_1h_2 + h_1h_3 + h_2h_3}_{2\text{ way}} + \underbrace{h_1h_2h_3}_{3\text{ way}} = h_2 + h_3 + h_2h_3 = 2(\mathsf{b} + \mathsf{d}) + (\mathsf{b} + \mathsf{d})^2.$$

Multiplying this polynomial by d for the $b \rightleftharpoons d$ transition gives

$$\mathsf{d}[2(\mathsf{b} + \mathsf{d}) + (\mathsf{b} + \mathsf{d})^2] = 2\mathsf{bd} + 2\mathsf{d}^2 + \mathsf{b}^2\mathsf{d} + 2\mathsf{bd}^2 + \mathsf{d}^3,$$

so the allosteric factor associated with transition $\mathsf{d} = (b, d)$ in context ad^2 is $\eta_{\mathsf{bd}}^2\eta_{\mathsf{dd}}^2\eta_{\mathsf{bbd}}\eta_{\mathsf{bdd}}^2\eta_{\mathsf{ddd}}$, in agreement with the previous calculation.

10. Discussion

The framework presented here for understanding allostery in receptor oligomers is an intriguing and novel combination of graph theory and quantitative receptor pharmacology. We began by establishing that the structure of state-transition diagram of a receptor k-mer, for any given monomer topology G, is the reduced graph power $G^{(k)}$. We showed that the equilibrium probabilities of a receptor k-mer may be expressed in terms of the parameters for an isolated monomer and emergent allosteric parameters, without approximation and without assuming independence of receptor monomers.

For clarity, we have used the (perhaps over-simple) ternary complex model dimer and tetramer as running examples, but the approach is completely general. For any given spanning tree T_G of a monomer state-transition diagram G that is of interest, the allosteric parameters can be enumerated by performing the symbolic calculations of (9.1) and (9.2) in a computer algebra system.

The example code is provided in the supporting material (Section S3) that performs the required algebraic calculations for any T_G and k specified by the user. The special case of a receptor dimer composed of two cubical ternary complex monomers is discussed in Sections S2 and S3.3.

We need not elaborate on the limitations of this theoretical framework for allostery in receptor oligomers. These are, for the most part, inherited from the limitations of the receptor modelling as practised by quantitative pharmacologists.

The identifiability of allosteric parameters (η_*) that emerge in receptor oligomer models is an important question that is beyond the scope of this paper. Presumably, identifiability will depend on whether (or not) parameters inherited from the monomer (κ_i) are fixed during the process of fitting allosteric parameters to experiment. An information criterion could be used to determine if it is legitimate to assume any given allosteric parameter has non-negligible effect ($\eta_* \neq 1$).

We hope this theoretical framework for receptor oligomer allostery will be valuable to investigators interested in pharmacological alteration of signalling via oligomeric GPCRs. It would be straightforward to apply this analysis of allosteric interactions to equilibrium oligomeric receptor modelling in contexts other than GPCRs (ligand-gated ion channels, receptor tyrosine kinases etc.). Extension of this framework to non-equilibrium steady states would allow its application to kinetic studies of multimeric enzymes, including the G protein activation/deactivation cycle of oligomeric GPCRs.

Acknowledgements

GDCS is grateful for numerous stimulating conversations with Ron Smith, Dan Borrus and Wenchong He. The minimal cycle basis construction for reduced graph powers that is presented in the supplemental materials (Sections S5–S8) was found in collaboration with Richard H. Hammack and its description is adapted from Hammack & Smith (2017).

References

Audet, M. & Bouvier, M. (2012) Restructuring G-protein-coupled receptor activation. *Cell*, **151**, 14–23.

Borroto-Escuela, D. O., Rodriguez, D., Romero-Fernandez, W., Kapla, J., Jaiteh, M., Ranganathan, A., Lazarova, T., Fuxe, K. & Carlsson, J. (2018) Mapping the interface of a GPCR dimer: a structural model of the A2A adenosine and D2 dopamine receptor heteromer. *Front. Pharmacol.*, **9**, 1–16.

Bouvier, M. (2001) Oligomerization of G-protein-coupled transmitter receptors. *Nat. Rev. Neurosci.*, **2**, 274–286.

Casadó, V., Cortés, A., Ciruela, F., Mallol, J., Ferré, S., Lluis, C., Canela, E. I. & Franco, R. (2007) Old and new ways to calculate the affinity of agonists and antagonists interacting with G-protein-coupled monomeric and dimeric receptors: the receptor-dimer cooperativity index. *Pharmac. Ther.*, **116**, 343–354.

Chandrashekar, J., Hoon, M. A., Ryba, N. J. & Zuker, C. S. (2006) The receptors and cells for mammalian taste. *Nature*, **444**, 288.

Christopoulos, A. & Kenakin, T. (2002) G protein-coupled receptor allosterism and complexing. *Pharmacol. Rev.*, **54**, 323–374.

Conn, P. J., Christopoulos, A. & Lindsley, C. W. (2009) Allosteric modulators of GPCRs: a novel approach for the treatment of CNS disorders. *Nat. Rev. Drug Discov.*, **8**, 41.

De Lean, A., Stadel, J. M. & Lefkowitz, R. J. (1980) A ternary complex model explains the agonist-specific binding properties of the adenylate cyclase-coupled beta-adrenergic receptor. *J. Biol. Chem.*, **255**, 7108–7117.

Di Cera, E. (2005) *Thermodynamic Theory of Site-Specific Binding Processes in Biological Macromolecules*. Cambridge University Press, Cambridge.

Durroux, T. (2005) Principles: a model for the allosteric interactions between ligand binding sites within a dimeric GPCR. *Trends Pharmacol. Sci.*, **26**, 376–384.

Eaton, W. A., Henry, E. R., Hofrichter, J., Bettati, S., Viappiani, C. & Mozzarelli, A. (2007) Evolution of allosteric models for hemoglobin. *IUBMB Life*, **59**, 586–599.

Ehlert, F. J. (2000) The ternary complex model. *Biomedical Applications of Computer Modeling* (A. Christopoulos). Handbooks in Pharmacology and Toxicology. CRC Press, pp. 21–85.

Engers, D. W. & Lindsley, C. W. (2013) Allosteric modulation of Class C GPCRs: a novel approach for the treatment of CNS disorders. *Drug Discov. Today Technol.*, **10**, e269–e276.

Farran, B. (2017) An update on the physiological and therapeutic relevance of GPCR oligomers. *Pharmacol. Res.*, **117**, 303–327.

Ferré, S. (2015) The GPCR heterotetramer: challenging classical pharmacology. *Trends Pharmacolog. Sci.*, **36**, 145–152.

Ferré, S., Ciruela, F., Canals, M., Marcellino, D., Burgueno, J., Casadó, V., Hillion, J., Torvinen, M., Fanelli, F., De Benedetti, P., Goldberg, S. R., Bouvier, M., Fuxe, K., Agnate, L. F., Lluis, C., Franco, R., Woods, A. (2004) Adenosine A2A-dopamine D2 receptor–receptor heteromers. Targets for neuro-psychiatric disorders. *Parkinsonism Relat. Disord.*, **10**, 265–271.

Ferré, S., Casadó, V., Devi, L. A., Filizola, M., Jockers, R., Lohse, M. J., Milligan, G., Pin, J.-P. & Guitart, X. (2014) G protein-coupled receptor oligomerization revisited: functional and pharmacological perspectives. *Pharmacol. Rev.*, **66**, 413–434.

Foster, D. J. & Conn, P. J. (2017) Allosteric modulation of GPCRs: new insights and potential utility for treatment of schizophrenia and other CNS disorders. *Neuron*, **94**, 431–446.

Fuxe, K., Marcellino, D., Leo, G. & Agnati, L. F. (2010) Molecular integration via allosteric interactions in receptor heteromers. A working hypothesis. *Curr. Opin. Pharmacol.*, **10**, 14–22.

Gaitonde, S. A. & González-Maeso, J. (2017) Contribution of heteromerization to G protein-coupled receptor function. *Curr. Opin. Pharmacol.*, **32**, 23–31.

Giraldo, J. (2012) Modeling cooperativity effects in dimeric G protein-coupled receptors. *Oligomerization and Allosteric Modulation in G-Protein Coupled Receptors* (T. Kenakin ed). Oxford: Academic Press, pp. 349–373.

González-Maeso, J. (2011) GPCR oligomers in pharmacology and signaling. *Mol. Brain*, **4**, 20.

González-Maeso, J. (2014) Family a GPCR heteromers in animal models. *Front. Pharmacol.*, **5**, 226.

Goudet, C., Kniazeff, J., Hlavackova, V., Malhaire, F., Maurel, D., Acher, F., Blahos, J., Prezeau, L. & Pin, J.-P. (2005) Asymmetric functioning of dimeric metabotropic glutamate receptors disclosed by positive allosteric modulators. *J. Biol. Chem.*, **280**, 24380–24385.

Gregory, K. J., Sexton, P. M. & Christopoulos, A. (2010) Overview of receptor allosterism. *Curr. Protoc. Pharmacol.*, **51**, 1–21.

Gregory, K. J., Noetzel, M. J. & Niswender, C. M. (2013) Pharmacology of metabotropic glutamate receptor allosteric modulators: structural basis and therapeutic potential for CNS disorders. *Prog. Mol. Biol. Transl. Sci.*, **115**, 61–121.

Hall, D. A. (2012) Application of receptor theory to allosteric modulation of receptors. *Oligomerization and Allosteric Modulation in G-Protein Coupled Receptors* (T. Kenakin ed). Oxford: Academic Press, pp. 217–290.

Hammack, R. & Smith, G. (2017) Cycle bases of reduced powers of graphs. *Ars Math. Contemp.*, **12**, 183–203.

Hill, T. L. (1989) *Free Energy Transduction in Biology and Biochemical Cycle Kinetics*. New York: Springer.

Hill, T. L. (1985) *Cooperativity Theory in Biochemistry: Steady-state and Equilibrium Systems*. New York: Springer.

Kaczor, A. & Selent, J. (2011) Oligomerization of G protein-coupled receptors: biochemical and biophysical methods. *Curr. Med. Chem.*, New York, **18**, 4606–4634.

Kenakin, T. (2004) Principles: receptor theory in pharmacology. *Trends Pharmacol. Sci.*, **25**, 186–192.

Kenakin, T. (2014) *Oligomerization and Allosteric Modulation in G-Protein Coupled Receptors*, vol. **115**, 1st edn. Progress in Molecular Biology and Translational Science. Academic Press.

Kenakin, T. (2016) Theoretical aspects of GPCR-ligand complex pharmacology. *Chem. Rev.*, **117**, 4–20.

Kenakin, T. (2018) *A Pharmacology Primer: Techniques for More Effective and Strategic Drug Discovery*. Academic Press, Oxford.

Kubo, Y. & Tateyama, M. (2005) Towards a view of functioning dimeric metabotropic receptors. *Curr. Opin. Neurobiol.*, **15**, 289–295.

Levitz, J., Habrian, C., Bharill, S., Fu, Z., Vafabakhsh, R. & Isacoff, E. Y. (2016) Mechanism of assembly and cooperativity of homomeric and heteromeric metabotropic glutamate receptors. *Neuron*, **92**, 143–159.

Maguire, M. E., van Arsdale, P. M. & Gilman, A. G. (1976) An agonist-specific effect of guanine nucleotides on binding to the beta adrenergic receptor. *Mol. Pharmacol.*, **12**, 335–339.

Marshall, F. H., Jones, K. A., Kaupmann, K. & Bettler, B. (1999) GABAB receptors—the first 7TM heterodimers. *Trends Pharmacol. Sci.*, **20**, 396–399.

May, L. T., Leach, K., Sexton, P. M. & Christopoulos, A. (2007) Allosteric modulation of G protein-coupled receptors. *Annu. Rev. Pharmacol. Toxicol.*, **47**, 1–51.

Milligan, G. & Smith, N. J. (2007) Allosteric modulation of heterodimeric G-protein-coupled receptors. *Trends Pharmacol. Sci.*, **28**, 615–620.

Milligan, G., Ward, R. J. & Marsango, S. (2019) GPCR homo-oligomerization. *Curr. Opin. Cell Biol.*, **57**, 40–47.

Niswender, C. M. & Conn, P. J. (2010) Metabotropic glutamate receptors: physiology, pharmacology, and disease. *Annu. Rev. Pharmacol. Toxicol.*, **50**, 295–322.

O'Brien, D. E. & Conn, P. J. (2016) Neurobiological insights from mGlu receptor allosteric modulation. *Int. J. Neuropsychopharmacol.*, **19**, 1–10.

Palczewski, K. (2010) Oligomeric forms of G protein-coupled receptors (GPCRs). *Trends Biochem. Sci.*, **35**, 595–600.

Park, P. S.-H. & Palczewski, K. (2005) Diversifying the repertoire of G protein-coupled receptors through oligomerization. *Proc. Natl. Acad. Sci. U. S. A.*, **102**, 8793–8794.

Park, P. S.-H., Filipek, S., Wells, J. W. & Palczewski, K. (2004) Oligomerization of G protein-coupled receptors: past, present, and future. *Biochemistry*, **43**, 15643–15656.

Park, P. S.-H., Lodowski, D. T. & Palczewski, K. (2008) Activation of G protein-coupled receptors: beyond two-state models and tertiary conformational changes. *Annu. Rev. Pharmacol. Toxicol.*, **48**, 107–141.

Pin, J.-P. & Bettler, B. (2016) Organization and functions of mGlu and GABA B receptor complexes. *Nature*, **540**, 60.

Pin, J.-P., Kniazeff, J., Binet, V., Liu, J., Maurel, D., Galvez, T., Duthey, B., Havlickova, M., Blahos, J., Prézeau, L. & Rondard, P. (2004) Activation mechanism of the heterodimeric GABAB receptor. *Biochem. Pharmacol.*, **68**, 1565–1572.

Rosenbaum, D. M., Rasmussen, S. G. F. & Kobilka, B. K. (2009) The structure and function of G-protein-coupled receptors. *Nature*, **459**, 356–363.

Rovira, X., Vivó, M., Serra, J., Roche, D., Strange, P. & Giraldo, J. (2009) Modelling the interdependence between the stoichiometry of receptor oligomerization and ligand binding for a coexisting dimer/tetramer receptor system. *Br. J. Pharmacol.*, **156**, 28–35.

Terrillon, S. & Bouvier, M. (2004) Roles of G-protein-coupled receptor dimerization: from ontogeny to signalling regulation. *EMBO Rep.*, **5**, 30–34.

Vischer, H. F., Castro, M. & Pin, J. P. R. (2015) G protein-coupled receptor multimers: a question still open despite the use of novel approaches. *Mol. Pharmacol.*, **88**, 561–571.

Wang, W., Qiao, Y. & Li, Z. (2018) New insights into modes of GPCR activation. *Trends Pharmacol. Sci.*, **39**, 367–386.

Weiss, J. M., Morgan, P. H., Lutz, M. W. & Kenakin, T. P. (1996) The cubic ternary complex receptor–occupancy model I. Model description. *J. Theor. Biol.*, **178**, 151–167.